Supplementary Information for "Mobile Exceptional Points Generate Momentum-Space Switching Domains"

Jung-Wan Ryu[1,2] and Chang-Hwan Yi[3,4,5,*]

[1] *Center for Trapped Ion Quantum Science, Institute for Basic Science (IBS), Daejeon 34126, Republic of Korea*
[2] *IBS school of Basic Science, Korea University of Science and Technology (UST), Daejeon 34113, Republic of Korea*
[3] *Center for Theoretical Physics of Complex Systems, Institute for Basic Science (IBS), Daejeon 34126, Republic of Korea*
[4] *Department of Physics, Pukyong National University, Busan 48513, Republic of Korea*
[5] *Department of Physics, Hanyang University, Seoul 04763, Republic of Korea*

CONTENTS

Page

Note 1. Analytic condition and geometric interpretation of the switching boundary — ii

Note 2. Numerical evaluation of the band-permutation invariant — iii

Note 3. EP trajectory in extended parameter space — iii

Note 4. EP regimes of the model — iv

Note 5. Additional examples of eigenvalue braiding — vii

Note 6. Supplementary movies — viii

* yichanghwan@hanmail.net

Note 1. ANALYTIC CONDITION AND GEOMETRIC INTERPRETATION OF THE SWITCHING BOUNDARY

The boundary separating switching and nonswitching regions can be obtained analytically from Eqs. (1) and (2) of the main text. EPs occur when the two eigenvalues coalesce, corresponding to the condition

$$\Delta(\mathbf{k}, \phi) = 0. \tag{S1}$$

Using Eq. (2) of the main text, this condition becomes

$$\epsilon_0^2 + (t_x + t_y)\left(t_x e^{ik_x} + t_y e^{ik_y} + \mu e^{i\phi}\right) = 0. \tag{S2}$$

Rearranging terms gives

$$\epsilon_0^2 + (t_x + t_y)(t_x e^{ik_x} + t_y e^{ik_y}) + (t_x + t_y)\mu e^{i\phi} = 0. \tag{S3}$$

Defining

$$C(\mathbf{k}) = \epsilon_0^2 + (t_x + t_y)(t_x e^{ik_x} + t_y e^{ik_y}), \tag{S4}$$

the EP condition can be written as

$$C(\mathbf{k}) + (t_x + t_y)\mu e^{i\phi} = 0. \tag{S5}$$

Since $|e^{i\phi}| = 1$, a solution for ϕ exists only when

$$|C(\mathbf{k})| = |t_x + t_y|\mu. \tag{S6}$$

This condition determines the set of momenta for which the spectral trajectory $\Delta(\mathbf{k}, \phi)$ reaches the origin of the complex plane for some value of ϕ. At these momenta the spectral gap closes and the winding number $W(\mathbf{k})$ can change, thereby defining the boundary between switching and nonswitching regions in the Brillouin zone.

Consequently, the switching boundary corresponds to the projection of EP trajectories in the extended parameter space (k_x, k_y, ϕ) onto the (k_x, k_y) plane. Across this boundary, the winding number $W(\mathbf{k})$ changes between 0 and 1.

This result can be further understood by explicitly evaluating the winding number. From Eq. (S5), the spectral quantity can be written as

$$\Delta^2(\mathbf{k}, \phi) = C(\mathbf{k}) + (t_x + t_y)\mu e^{i\phi}, \tag{S7}$$

which describes a circular trajectory in the complex plane centered at $C(\mathbf{k})$ with radius $|(t_x + t_y)\mu|$.

When $|C(\mathbf{k})| < |(t_x + t_y)\mu|$, the trajectory of $\Delta^2(\mathbf{k}, \phi)$ encloses the origin during one modulation cycle, yielding $W(\mathbf{k}) = 1$.

In contrast, when $|C(\mathbf{k})| > |(t_x + t_y)\mu|$, the trajectory does not enclose the origin, yielding $W(\mathbf{k}) = 0$.

Therefore, the condition $|C(\mathbf{k})| = |(t_x + t_y)\mu|$ determines the switching boundary, separating the regions with $W(\mathbf{k}) = 1$ and $W(\mathbf{k}) = 0$.

Note 2. NUMERICAL EVALUATION OF THE BAND-PERMUTATION INVARIANT

In the numerical calculations presented in the main text, the band-permutation invariant $W(\mathbf{k})$ is obtained from the winding of $\Delta^2(\mathbf{k}, \phi)$ during one modulation cycle. To ensure a well-defined invariant, we evaluate the winding using the squared quantity $\Delta^2(\mathbf{k}, \phi)$, which is single-valued over the cycle. For each momentum point $\mathbf{k}$, the control parameter ϕ is discretized over the interval $[0, 2\pi]$, and the complex quantity $\Delta^2(\mathbf{k}, \phi)$ is evaluated along the cycle.

The invariant is computed from the phase winding of $\Delta^2(\mathbf{k}, \phi)$ around the origin of the complex plane,

$$W(\mathbf{k}) = \frac{1}{2\pi} \oint d\phi\, \partial_\phi \arg\left[\Delta^2(\mathbf{k}, \phi)\right]. \tag{S8}$$

In practice, this winding number is evaluated numerically using a discretized phase accumulation,

$$W(\mathbf{k}) = \frac{1}{2\pi} \sum_j \arg\left[\frac{\Delta^2(\mathbf{k}, \phi_{j+1})}{\Delta^2(\mathbf{k}, \phi_j)}\right], \tag{S9}$$

where the phase difference is obtained from the argument of the complex ratio.

A winding number $W(\mathbf{k}) = 1$ indicates that $\Delta^2(\mathbf{k}, \phi)$ encloses the origin in the complex plane, corresponding to a sign change of $\Delta(\mathbf{k}, \phi)$ after one modulation cycle and hence eigenmode exchange. In contrast, $W(\mathbf{k}) = 0$ indicates that the trajectory does not enclose the origin and therefore no band permutation occurs. This numerical procedure is used to construct the momentum-space maps of $W(\mathbf{k})$ presented in Fig. 2 of the main text. The discretization of the modulation cycle was chosen sufficiently fine to ensure convergence of the winding number.

Note 3. EP TRAJECTORY IN EXTENDED PARAMETER SPACE

To visualize the origin of the switching domains, we analyze the motion of EPs in the extended parameter space (k_x, k_y, ϕ). The EP condition yields two solution branches that trace continuous trajectories as ϕ evolves from 0 to 2π. Figure S1 shows the resulting EP trajectories for the same parameter regimes as those used in Fig. 2 of the main text. As ϕ varies, the EPs move through the Brillouin zone and form curves in the extended parameter space. Open circles mark collision points where the two EPs merge and annihilate or reappear through pair creation.

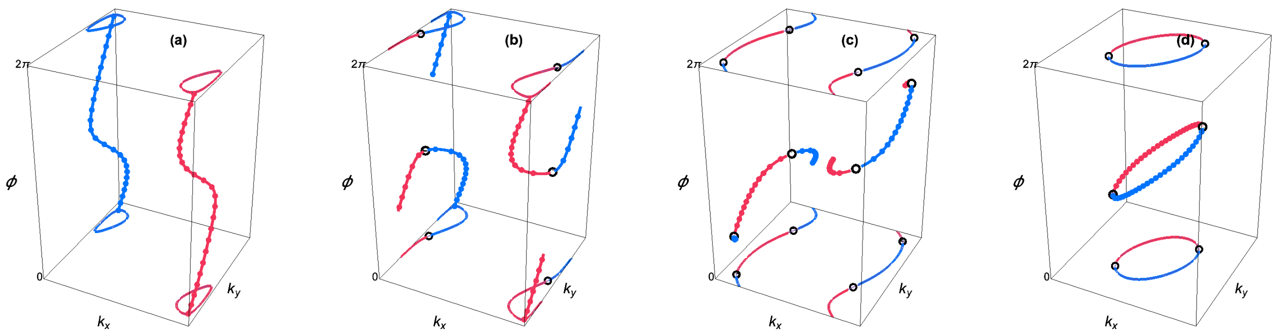

FIG. S1. Trajectories of EPs in the extended parameter space (k_x, k_y, ϕ). Blue and red curves denote the two EP branches as the cyclic control parameter ϕ varies from 0 to 2π. Open circles indicate pair-annihilation and pair-creation points where the two EPs merge and disappear or re-emerge. Panels (a-d) correspond to the same parameter regimes as in Fig. 2 of the main text. The projections of these trajectories onto the (k_x, k_y) plane coincide with the switching-domain boundaries of the band-permutation invariant $W(\mathbf{k})$.

Note 4. EP REGIMES OF THE MODEL

To illustrate the different spectral regimes of the model, we examine representative Riemann surfaces of the complex energy spectrum. In the numerical calculations shown in Supplementary Figs. S2 and S3 we use the representative parameters $t_x = 1$, $t_y = 0.5$, and $\epsilon_0 = 1.2$. Supplementary Fig. S2 shows two limiting cases of the modulation amplitude μ. For sufficiently small μ, two EPs are present in the Brillouin zone for all values of the cyclic parameter ϕ. In this regime the two sheets of the spectrum are connected through branch cuts terminating at the EPs. In contrast, for sufficiently large μ the spectrum remains fully gapped and no EPs exist in the Brillouin zone. In this case the two sheets of the spectrum remain disconnected.

EPs occur when the eigenvalue discriminant of the Hamiltonian vanishes, i.e., when the two complex eigenvalues become degenerate. For the present model this condition can be written as

$$|t_x - t_y| \leq \left| \frac{\epsilon_0^2}{t_x + t_y} + \mu e^{i\phi} \right| \leq t_x + t_y.$$

For the parameters used in this work this condition becomes

$$0.5 \leq |0.96 + \mu e^{i\phi}| \leq 1.5.$$

This inequality defines an annular region in the complex plane of the parameter $0.96 + \mu e^{i\phi}$. EPs exist only when the circular trajectory of this parameter intersects this annulus as ϕ varies from 0 to 2π.

For the present parameters the structure of EPs changes at two characteristic modulation amplitudes. When $\mu < 0.46$, the circular trajectory remains entirely inside the annulus and two EPs exist for all values of ϕ. When $\mu > 2.46$, the trajectory lies completely outside the annulus and the spectrum remains fully gapped throughout the

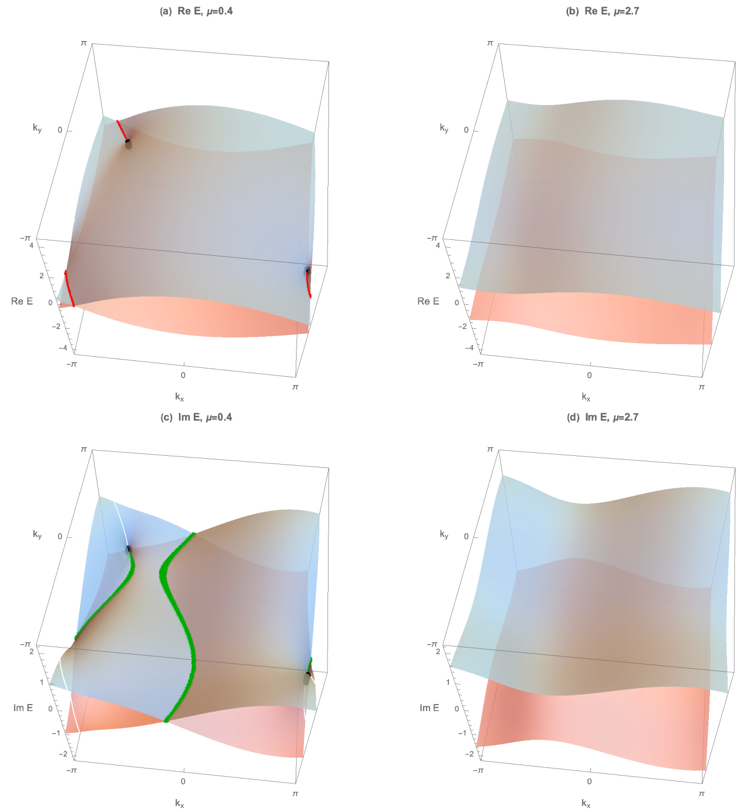

FIG. S2. Limiting spectral regimes for small and large μ, corresponding to the presence and absence of EPs. (a,c) For $\mu = 0.4$, two EPs are present in the Brillouin zone and the two sheets of the spectrum are connected by branch cuts terminating at the EPs. (b,d) For $\mu = 2.7$, the spectrum remains fully gapped and no EPs occur, so the two sheets remain disconnected. Red (green) points indicate the loci where the real (imaginary) part of the band gap vanishes, corresponding to the branch cuts of the real (imaginary) Riemann surfaces, while black points denote EPs. All panels are calculated for $t_x = 1$, $t_y = 0.5$, and $\epsilon_0 = 1.2$ with $\phi = \pi/2$.

TABLE S1. EP structure during the modulation cycle $\phi : 0 \to 2\pi$ for representative values of μ used in Fig. 2.

μ	EP structure during the cycle
0.4	EPs present for all ϕ
0.5	EPs present for $0 \le \phi < 2.86$ and $3.43 < \phi \le 2\pi$; no EPs for $2.86 < \phi < 3.43$
0.9	EPs present for $1.27 < \phi < 2.60$ and $3.68 < \phi < 5.02$; no EPs otherwise
2.0	EPs present for $2.34 < \phi < 3.94$; no EPs otherwise

entire modulation cycle. In the intermediate regime $0.46 < \mu < 2.46$, the trajectory intersects the annulus only within finite intervals of ϕ, leading to the creation and annihilation of EP pairs during the cycle.

For representative values of the modulation amplitude used in Fig. 2, Table S1 summarizes the presence or absence of EPs during the modulation cycle $\phi : 0 \to 2\pi$. These intervals can be directly compared with the EP trajectories shown in Supplementary Fig. S1.

The branch cuts visible in the spectral surfaces originate from the multi-valued nature of the complex eigenvalues

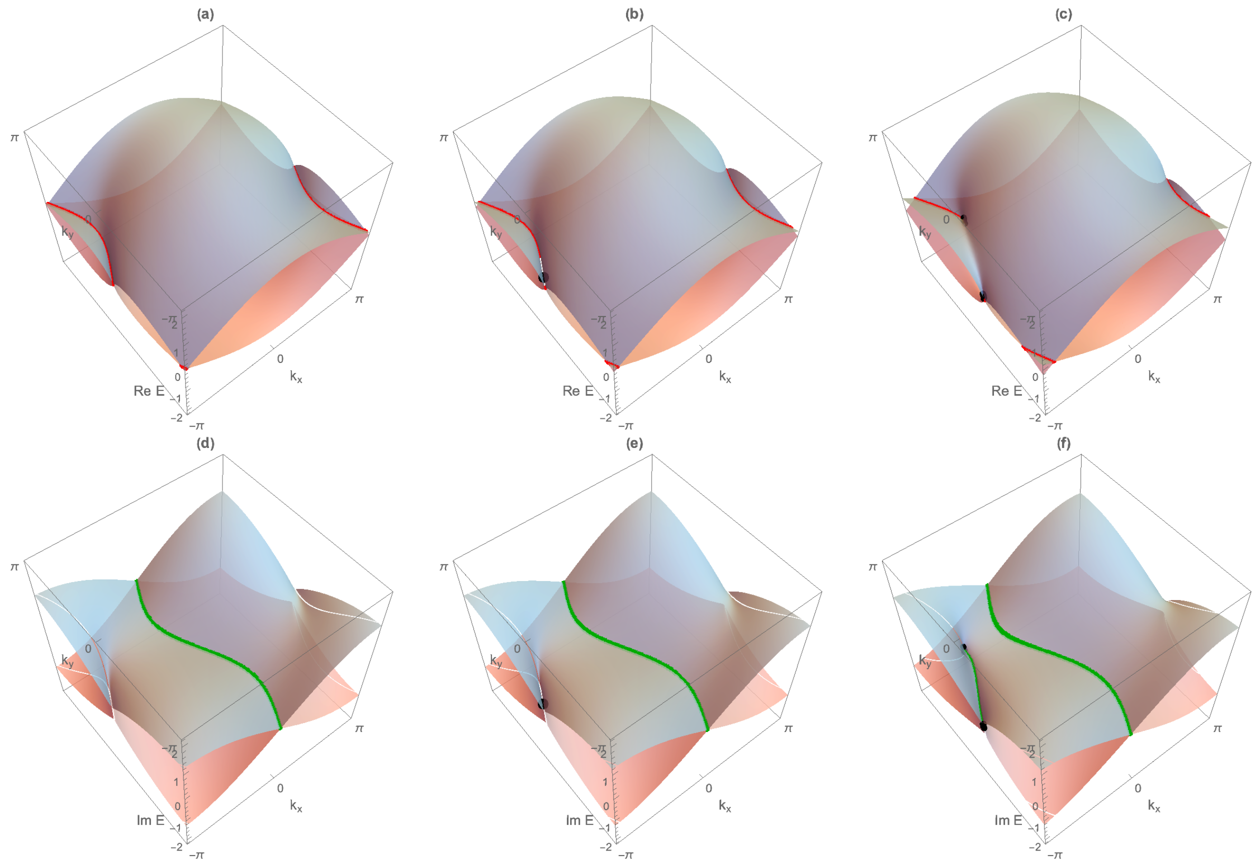

FIG. S3. EP annihilation and recreation near the transition for $\mu = 0.5$. (a,d) At $\phi = 3.0$, the spectrum is fully gapped and no EPs are present. (b,e) At the critical value $\phi = 2.8578$, the gap closes at a single momentum point. (c,f) At $\phi = 2.4$, a pair of EPs is present and the two sheets of the spectrum are connected by branch cuts terminating at the EPs. Red (green) points indicate the loci where the real (imaginary) part of the band gap vanishes. All panels use the parameters $t_x = 1$, $t_y = 0.5$, $\epsilon_0 = 1.2$, and $\mu = 0.5$.

near EPs. They represent the loci in momentum space where the real or imaginary part of the band gap vanishes, thereby connecting the two sheets of the Riemann surface.

As ϕ varies during the modulation cycle, the EPs move through the Brillouin zone and may annihilate or reappear depending on the value of μ. Supplementary Fig. S3 illustrates this process for $\mu = 0.5$. In the panels shown there, the spectrum is fully gapped at $\phi = 3.0$, the gap closes at the critical value $\phi = 2.8578$, and two EPs are present at $\phi = 2.4$. This evolution reflects the annihilation or recreation of an EP pair as the cyclic parameter is varied.

These results demonstrate that the switching-domain structure discussed in the main text originates from the geometric motion of EPs in the extended parameter space (k_x, k_y, ϕ). As the control parameter ϕ evolves during the cycle, the EPs move through momentum space and reorganize the spectral Riemann surface.

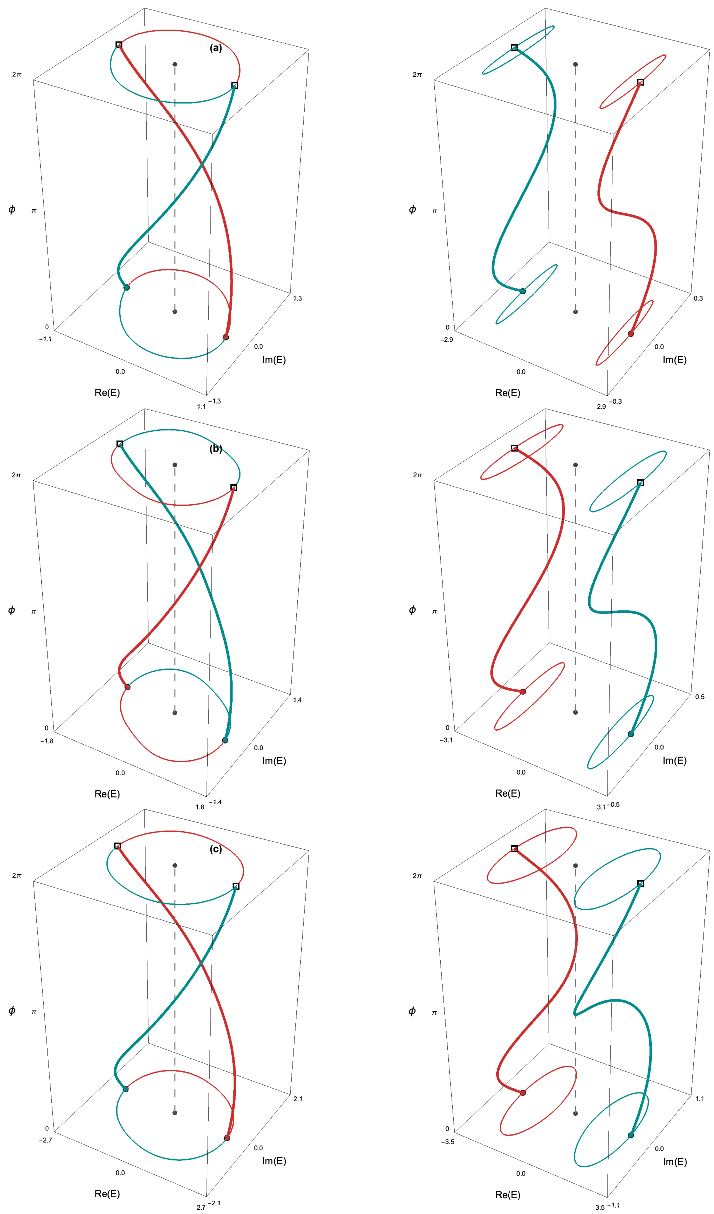

FIG. S4. Complex-energy braiding for representative momentum points corresponding to the domain configurations in Fig. 2(b)–(d). Panels (a), (b), and (c) correspond to representative momentum points from the domain configurations shown in Fig. 2(b), Fig. 2(c), and Fig. 2(d), respectively. For each value of μ, the left panel shows a momentum point with $W(\mathbf{k}) = 1$, while the right panel shows a point with $W(\mathbf{k}) = 0$. The solid curves represent the eigenvalue trajectories in the three-dimensional space $(\mathrm{Re}E, \mathrm{Im}E, \phi)$ during one modulation cycle $\phi : 0 \to 2\pi$. Filled circles indicate the eigenvalues at $\phi = 0$, and open squares indicate the eigenvalues at $\phi = 2\pi$. For $W(\mathbf{k}) = 1$, the trajectories encircle the origin, resulting in an exchange of eigenmodes after the cycle, whereas for $W(\mathbf{k}) = 0$, the trajectories do not enclose the origin and the eigenvalues return to their original branches.

Note 5. ADDITIONAL EXAMPLES OF EIGENVALUE BRAIDING

In the main text we demonstrated the relation between the band-permutation invariant and eigenvalue braiding using representative momentum points corresponding to the domain structure in Fig. 2(a). Here we provide additional examples corresponding to the domain configurations shown in Fig. 2(b)–(d).

Figure S4 shows the complex-energy trajectories for representative momentum points with $W(\mathbf{k}) = 1$ and $W(\mathbf{k}) = 0$. These examples further confirm that the invariant $W(\mathbf{k})$ determines whether eigenvalue braiding occurs during cyclic modulation. The eigenvalue branches are tracked continuously along the modulation cycle by matching eigenvalues between neighboring ϕ steps in the complex-energy plane.

Note 6. SUPPLEMENTARY MOVIES

To provide a direct visualization of the spectral evolution discussed in the main text, we provide two sets of animations illustrating the motion of EPs and the resulting evolution of the spectral Riemann surfaces during one modulation cycle of the control parameter ϕ.

These movies provide a direct visualization of the geometric origin of the switching domains, where the boundaries correspond to the projection of EP trajectories in the extended parameter space (k_x, k_y, ϕ) onto the (k_x, k_y) plane.

Movies S1–S5: EP motion and branch-cut evolution in the Brillouin zone.

These animations show the motion of EPs and the corresponding branch cuts in the Brillouin zone as the control parameter ϕ varies from 0 to 2π. The black curves denote the boundaries of the switching domains determined by the band-permutation invariant $W(\mathbf{k})$. Red and green curves indicate the real and imaginary branch cuts, respectively, and black points denote EPs. The red and blue regions correspond to momentum-space domains where band permutation occurs ($W = 1$) and does not occur ($W = 0$). These animations illustrate how the motion of EPs and the accompanying evolution of branch cuts in the Brillouin zone generate the switching-domain structure in momentum space.

Movie S1: $\mu = 0.4$ (`mu0.4_animation.gif`)

Movie S2: $\mu = 0.5$ (`mu0.5_animation.gif`)

Movie S3: $\mu = 0.9$ (`mu0.9_animation.gif`)

Movie S4: $\mu = 2.0$ (`mu2.0_animation.gif`)

Movie S5: $\mu = 2.7$ (`mu2.7_animation.gif`)

Movies S6–S10: Evolution of the complex band structure.

These animations show the real and imaginary parts of the complex bands during one modulation cycle of ϕ for representative values of the modulation amplitude μ. The two bands are displayed as surfaces over the Brillouin zone together with the positions of EPs and the corresponding branch cuts, illustrating how the Riemann-surface structure evolves as ϕ varies.

In each animation two representative momentum points are tracked. The orange marker denotes a point located inside the band-permutation domain, while the blue marker denotes a point outside this domain. As ϕ evolves over one cycle, the tracked eigenmode at the orange point moves from one band to the other, demonstrating band permutation. In contrast, the eigenmode at the blue point returns to the same band after the cycle.

Movie S6: $\mu = 0.4$ (`riemann_real_imag_animation_mu0.4.gif`)

Movie S7: $\mu = 0.5$ (`riemann_real_imag_animation_mu0.5.gif`)

Movie S8: $\mu = 0.9$ (`riemann_real_imag_animation_mu0.9.gif`)

Movie S9: $\mu = 2.0$ (`riemann_real_imag_animation_mu2.0.gif`)

Movie S10: $\mu = 2.7$ (`riemann_real_imag_animation_mu2.7.gif`)